FEBS Letters 567 (2004) 20–26 FEBS 28303

Minireview

Ribosomal crystallography: a flexible nucleotide anchoring tRNA translocation, facilitates peptide-bond formation, chirality discrimination and antibiotics synergism

Ilana Agmon[a], Maya Amit[a], Tamar Auerbach[a,b], Anat Bashan[a], David Baram[a,b], Heike Bartels[b], Rita Berisio[b,1], Inbal Greenberg[a], Joerg Harms[b], Harly A.S. Hansen[b], Maggie Kessler[a], Erez Pyetan[a,b], Frank Schluenzen[b], Assa Sittner[a], Ada Yonath[a,b,*], Raz Zarivach[a]

[a] *Department of Structural Biology, The Weizmann Institute, 76100 Rehovot, Israel*
[b] *Max-Planck-Research Unit for Ribosomal Structure, 22603 Hamburg, Germany*

Received 11 March 2004; accepted 14 March 2004

Available online 8 April 2004

Edited by Horst Feldmann

Abstract The linkage between internal ribosomal symmetry and transfer RNA (tRNA) positioning confirmed positional catalysis of amino-acid polymerization. Peptide bonds are formed concurrently with tRNA-3′end rotatory motion, in conjunction with the overall messenger RNA (mRNA)/tRNA translocation. Accurate substrate alignment, mandatory for the processivity of protein biosynthesis, is governed by remote interactions. Inherent flexibility of a conserved nucleotide, anchoring the rotatory motion, facilitates chirality discrimination and antibiotics synergism. Potential tRNA interactions explain the universality of the tRNA CCA-end and P-site preference of initial tRNA. The interactions of protein L2 tail with the symmetry-related region periphery explain its conservation and its contributions to nascent chain elongation.

Keywords: Ribosome; Peptide-bond formation; Positional catalysis; Antibiotics synergism; Synercid; Azithromycin; Dual binding

1. Introduction

Ribosomes are the cellular organelles catalyzing polymerization of amino acids according to the genetic code sequence, encoded in messenger RNA (mRNA). Transfer RNA (tRNA) molecules carry the amino acids, esterified to their 3′ends, which consists of the universally conserved single-stranded sequence CCA. Ribosomes possess three tRNA binding sites, A, P and E, hosting the aminoacyl, peptidyl-tRNA and the exiting tRNA, respectively. Each elongation cycle involves the advancement of the mRNA together with A → P → E-site passage of the tRNA molecules, driven by GTPase activity. Ribosomes are composed of two subunits of unequal size, which associate to produce a functional ribosome. Within the functionally active ribosome, the small subunit interacts with the tRNA anticodon triplet and the large subunit provides the peptidyl transferase center (PTC) center and the path for the nascent protein, hence interacting with the tRNA acceptor stem and its CCA end. Analysis of the available ribosomal structures of eubacteria [1–4] and archaea [5] showed that both the decoding site and the PTC consist exclusively of ribosomal RNA (rRNA). Being the main player in a fundamental cell process, the ribosome is targeted by many clinically relevant antibiotics. These were shown to hamper protein biosynthesis by limiting ribosomal mobility, by blocking the progression of nascent proteins or by perturbing the architecture of the ribosomal active centers.

Here, we discuss the linkage between the spectacular ribosomal architecture, its crucial conformational mobility and antibiotics synergism. We also address positional catalysis of peptide-bond formation and nascent chain elongation, chirality discrimination, the universality of the tRNA CCA end and the possible contribution of a ribosomal protein to partial stabilization of the dynamic PTC.

2. Positional catalysis

The PTC is located in the large subunit, close to the subunit interface, at the bottom of a cavity (Fig. 1(a)) that opens into a long tunnel that spans the large subunit and serves as the path taken by nascent peptides until they emerge out of the ribosome. The PTC crevice and its environment are located in the midst of a sizable symmetry-related region, containing about 180 nucleotides, revealed by us in all known structures of the large ribosomal subunit (Fig. 1(b)) [3–15]. This unique symmetrical region within the otherwise asymmetrical ribosome relates the RNA backbone fold and the nucleotides orientations, rather than their types. It encapsulates the PTC, and its symmetry axis that passes midway between the A and the P loops, almost coincides with the long axis of the protein exit tunnel [11,16–18]. The requirement to offer comparable supportive environments to two similar chemical moieties in an

* Corresponding author. Fax: +972-8-934-4154.
E-mail address: ada.yonath@weizmann.ac.il (A. Yonath).

[1] Permanent address: Institute of Biostructure and Bioimaging, CNR, 80138 Naples, Italy.

0014-5793/$22.00 © 2004 Published by Elsevier B.V. on behalf of the Federation of European Biochemical Societies.
doi:10.1016/j.febslet.2004.03.065

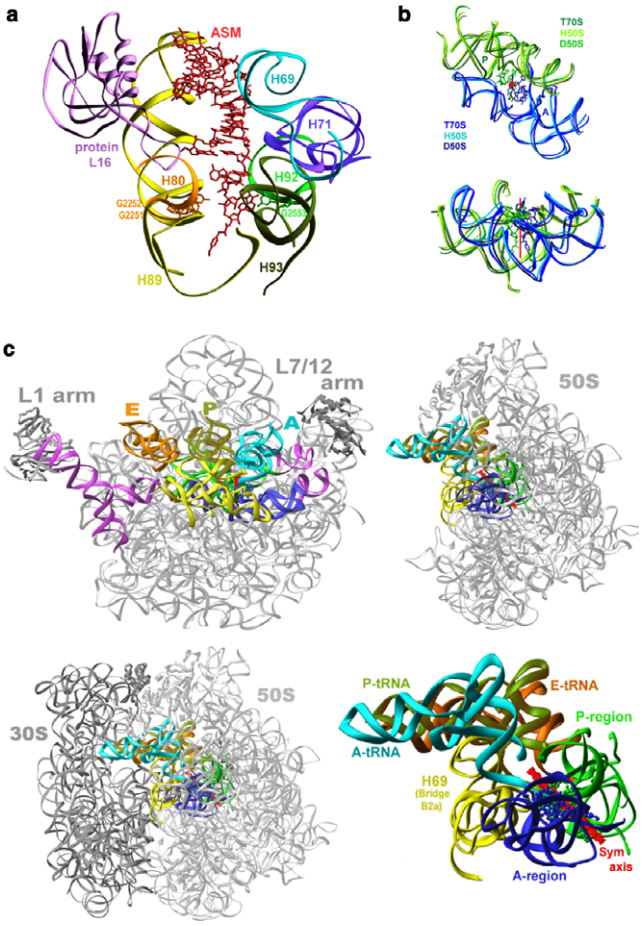

Fig. 1. (a) The D50S PTC cavity viewed from the subunit interface, together with ASM, a 35 nucleotides substrate analog mimicking the A-site tRNA acceptor stem and its aminoacylated 3′end [11]. The nucleotides known to form basepairs with tRNA molecules are marked by their numbers. (b) Two perpendicular views of the RNA backbone of the symmetry related region in all known structures [3–5]. The symmetry axis is red. The bottom view shows also the ASM 3′end (at the A-site, in blue) and the derived P-site 3′end (in green), both shown as atoms. (c) The position of the symmetry related region within the large subunit. Its connections with the tRNA entrance and exit regions, as well as with the decoding site in the small subunit, are colored (in purple). Also shown are the docked three tRNA molecules, bound to the whole ribosome [3], as well as the 3′ends of ASM and the derived P-site tRNA. In all, the rRNA backbone is shown as gray ribbons. Top panel: The front (left) and side (right) views of D50S. Bottom left includes the small subunit, as determined within the entire ribosomes [3]. Bottom right shows the colored features in all other views, including the symmetry related region, its axis, Helix H69 and the docked tRNA molecules. Note the strategic location of H69, consistent with its major contribution to the accurate placement of A-site tRNA, and to its presumed function in translocation [16,17,31].

orientation allowing peptide-bond formation, justifies the internal symmetry [18]. This symmetry-related region connects, directly or through its extensions, all functional regions of the large subunit, namely the tRNA entrance and exit sites, the PTC, the protein exit tunnel, with the decoding center in the small subunit (via the intersubunit bridge B2a, which is the tip of Helix H69) (Fig. 1(c)). Its central location suggests that it provides an intra-ribosomal functional signaling system between remote functional locations, essential for smooth processivity of amino-acids polymerization.

We found that for substrates that are positioned accurately, the bond connecting the aminoacylated tRNA-3′end to the rest of the tRNA molecule coincides with the symmetry axis of the symmetry-related region. Thus, it appears that tRNA translocation consists of two correlated movements: a rotation of the tRNA single-stranded terminus and a shift of the tRNA helical regions combined with the mRNA progression at the decoding site (Fig. 2(a)) [11,17]. An additional mechanistic element of the rotatory motion is its spiral nature. Thus, four

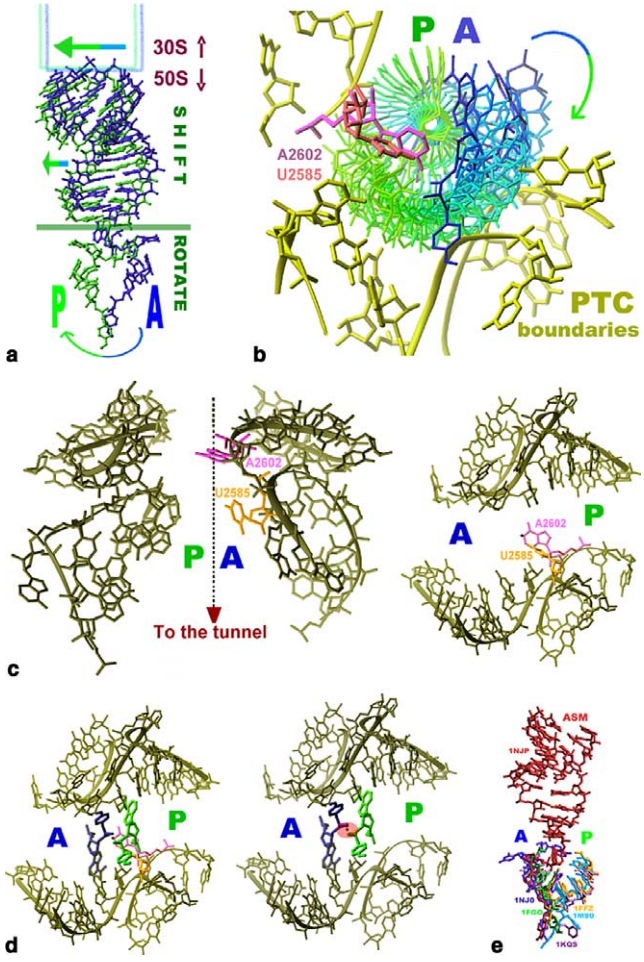

Fig. 2. (a) A translocating tRNA, from A-(blue) to P-(green) site. The dark green line shows the division between the double helical region that is being shifted (above the line) and the rotating 3′end (below), based on ASM position within D50S. As ASM [11] binds only to the large subunit, the tRNA regions that interact with the small subunit are represented by hollow blue-green boxes. The straight arrows show the shifting direction, and the round one represents the rotatory motion. (b–d) The PTC boundaries scaffolding the path of the rotatory motion. The positions of A2602 and U2585 are marked. (b) The right panel of (c) and (d) show views down the symmetry axis, from the tunnel towards the PTC. The right side of (c) is a view along the symmetry axis. In (b) the rotatory motion is represented by the gradual transfer from blue (A) to green (P) site. The figure shows snapshots of the rotatory motion, obtained by successive rotations from A-to P-site of the rotating moiety by 15° each, around the bond connecting the 3′end with the rest of the tRNA molecule. (d) Shows the position of the adenylated A76 of the tRNA at the A-site (as in ASM) and its derived P-site. The atoms involved in the actual peptide bond process are highlighted on the right. (e) A superposition of several substrate analogs, as observed in H50S [19] and D50S [11]. Note the similarity in the positions and the differences in the orientations.

P-region nucleotides positioned somewhat deeper in the PTC compared to their A-site mates appear to guide the nascent chain into the exit tunnel [11,17].

The PTC is an arched void of an architecture specifically designed for the A- to P-site rotatory motion, as its dimensions and shape are suitable to accommodate tRNA-3′ends throughout this passage and its boundaries create the template along which the rotating moiety slides (Fig. 2(b)) [11]. Two conserved nucleotides, A2602 (*Escherichia coli* numbering system is used throughout) and U2585 bulging from the PTC wall into its center, appear to provide a double-anchor for this motion (Figs. 2(b)–(d)) [11]. Guided by the rRNA scaffold along an exact pattern, the rotatory motion leads to stereochemistry optimal for peptide-bond formation (Fig. 2(d)), which seems to occur concurrently with the rotatory motion. This stereochemistry allows an A-site primary amine nucleophilic attack on the P-site tRNA carbonyl-carbon. This reaction should readily take place at the pH found to be optimal for protein biosynthesis (~7.5), which is close to the pH within D50S-complex crystals, the system exploited for the determination of the peptide-bond formation mechanism [11].

It seems, therefore, that the primary catalytic activity of the ribosome is the provision of an ingeniously designed structural framework, capable of guaranteeing smooth amino-acid polymerization. Composed of the structural components crucial for accurate tRNA substrates alignment, translocation along a guided template, and the entrance of the polypeptide into the exit tunnel, this framework is located in a central ribosomal region, interacting with all its functional domains, and appears to facilitate transfer of information between them. Hence, we concluded that the ribosome performs its dual catalytic tasks: peptide-bond formation and amino-acid polymerization by positioning catalysis [20,21], rather than by participating in actual chemical events, as suggested previously based on the crystal structure of a complex of H50S and a compound supposed to mimic an intermediate state analog [6,19].

The geometrical requirement for the ribosomal positional catalysis, apart from correctly positioned A-site tRNAs, is that the initial 3′end of the P-site tRNA adopts the flipped orientation. Some directionality for P-site positioning could be provided by the initial amino acid, consistent with its universality (f-met in prokaryotes or methionine in eukaryotes). Additionally, the tRNA anticodon loop in the initiation complex is bound to the P-site of the small subunit. Nevertheless, theoretically the flexible tRNA-3′end could be accommodated in various orientations at any position in the PTC, since at the beginning of protein synthesis both A and P sites are available. It appears that in order to prevent false binding, hence avoiding time consuming rearrangements, the P-site PTC possesses an extra potential candidate for basepairing, namely G2252 that can pair with tRNA-C74 [22], in addition to the symmetrical basepair with tRNA-C75 (Fig. 1(a)). The significance of this P-region double basepair combination, together with the preference of tRNA synthetases for aminoacyladenylates [23], rationalize the universality of the CCA motif in tRNA-3′end.

Additional deviations from the twofold symmetry at the PTC are associated with its dynamics. Owing to its tasks, the A-region possesses more mobility than the rather passive P-site. The larger number of the intra-region interactions within the P-region [18], together with the interactions of the outer region of the P-region with the tail of protein L2 [18], could be responsible for this unbalanced stabilization. The necessity of protein L2 for the elongation of nascent polypeptides [24], contrary to the ability of protein-free 23S rRNA to form single peptide bonds [25], is consistent with the difference between these two stages of protein biosynthesis. Thus, single peptide bonds can be formed even by approximately placed reactants, as observed in the crystal structure of a complex of the large ribosomal subunit from *Haloarcula marismortui*, H50S [8,19], whereas the rotatory motion that leads to elongation can be performed only within a well-outlined pattern, hence necessitating an exact placement in a stable framework.

3. Accurate substrate placement within a mobile PTC

A striking net of interactions between the tRNA acceptor stem and the PTC cavity upper rims (Fig. 1(a)) was observed in a complex of *Thermus thermophilus* ribosome, T70S, [3] and of unbound large subunit from *Deinococcus radiodurans*, D50S, with tRNA acceptor stem mimics [11]. In contrast to the dense network of substrate interactions with the upper rim of the PTC cavity, only a few contacts were detected within the PTC itself. Among these is the [26] Watson-Crick basepair between the A-region G2553 with tRNA C75, which was detected in all known structures of functional complexes [6,8,10,11]. This particular basepair was found to be created by tRNA mimics that bind to the PTC in a similar position, albeit having distinctly different orientations (Fig. 2(e)), all requiring conformational rearrangements for participating in peptide-bond formation [19]. Inaccurate binding may occur for puromycin derivatives that are too short to reach the upper rims of the PTC cavity; or when key constituents of the upper rims, responsible for the remote interactions (e.g., the tip of H69) are disordered, as is the case of crystal structure of H50S [5,6]. It seems, therefore, that the global localization of the tRNA molecules is dictated by the match between the overall ribosomal architecture and the size and shape of the tRNA molecules; that the universal basepair provides approximate anchoring even to short substrates, and that the precise substrate alignment is dominated by the remote interactions of the tRNA double helical acceptor stem with the distant rims of the PTC [20,21].

The diversity of binding modes observed within the PTC (summarized in [19–21]) demonstrates the relative ease of accommodating compounds resembling tRNA-3′end within the PTC, and of the formation of single peptide bonds by substrate analogs positioned in different orientations [8,19] manifests the PTC mobility. Inherent PTC conformational tolerance is required for its participation in the dynamic events associated with peptide-bond formation, and PTC conformational variability could be correlated to the functional state of the ribosome, which is, in turn, linked to environmental variations [27–30]. Similarly, the various PTC conformations observed in the various crystal structures [3,4,6] could be linked to the functional activity of the crystallized particles, hence to the relation between physiological and crystallization conditions [4,31].

Comparisons of known PTC conformations [3–15] indicated possible exploitation of the PTC flexibility for repositioning of less well-placed substrates [20,21]. A prominent candidate for this purpose is A2602, the universal nucleotide proposed to propel the rotatory motion of the tRNA-3′end in concert with

the overall translocation shift, presumably assisted by the tip of helix H69 [16,20,21,31] (Fig. 1(c)). A2602 is located at the center of the PTC close to the symmetry axis (Fig. 2(c)) and was shown to adopt various orientations [11,16,17]. Benefiting from its mobility, A2602 can assist the post-binding reorientation of approximately bound substrate analogs, a process bound to consume time, consistent with the lower rate of peptide-bonds formation by short puromycin derivatives, called the ''fragment reaction'', compared to normal protein biosynthesis [19]. Accordingly, our analysis revealed that additional structural requirements have to be fulfilled for subjecting the product of the reactions to chain elongation, consistent with the detection of a dipeptide, formed within H50S crystals, in the A-site of the PTC [8,19]. These observations demonstrate that remote interactions dominate productive substrate positioning and that accurate substrate alignment, mandatory for efficient peptide-bond formation and chain elongation, is achieved by the remote interactions despite the PTC flexibility.

4. U2585 is involved in anchoring the rotatory motion, in D-isomer elimination and in antibiotics synergism

Despite the PTC flexibility and its tolerance to non-productive substrate placements, it does not allow deviation from the chirality of its product, the protein. Normally, the tRNA molecules carry L-amino acids, thus dictating the L-configuration of the nascent proteins. However, the existence of minute amounts of D-amino acids could lead to mistakes. The exclusiveness of L-amino acids in proteins suggests the existence of ribosomal mechanism for avoiding D-isomer incorporation. Modeling attempts revealed two possible mechanisms: D-isomers rejection by spatial limitations, and the possibility to lock U2585 in a non-productive conformation (Fig. 3(a)) [32]. These results are consistent with the suggestion that D-amino acid incorporation can occur only under substantial conformational rearrangements [33] that may bypass both mechanisms.

U2585 is the nucleotide anchoring the rotatory motion [11,16,17] by direct interaction with the amino acid bound to the CCA. This universally conserved nucleotide plays a major role in protein biosynthesis, consistent with the dominant lethal phenotypes produced by its mutations [18]. Besides anchoring the rotatory motion and guaranteeing the proper chirality, it has a pivotal role in proper positioning of P-site substrates [34–38], a prerequisite for the formation of functional ribosomes. It may also influence, in a still unknown mechanism, the entrance of the newly formed peptides to the protein exit tunnel. Inherent conformational mobility enabling discrimination during selected steps of protein biosynthesis, as suggested for the nucleotide U2585, has been identified also in the ribosomal exit tunnel. Thus, under conditions unfavorable for the maturation of a nascent protein, specific sequences, associated with elongation arrest, appear to cause the tip of the β-hairpin of protein L22 to swing across the tunnel [12].

The protein exit tunnel is the preferred target of anti-microbial drugs from the macrolide and ketolides families, and crystallographic studies, using D50S as a pathogen model demonstrated unambiguously that clinically relevant amounts of these antibiotics block the tunnel and interfere with nascent chain progression (Fig. 3(b)) [7,12–15,39]. Streptogramins are unique among the ribosome-targeting antibiotics, since they consist of two components (A and B) that act synergistically [40] converting weak bacteriostatic effects into lethal bactericidal activity. Each compound has a moderate bacteriostatic activity, but their combination is quite powerful, displaying a

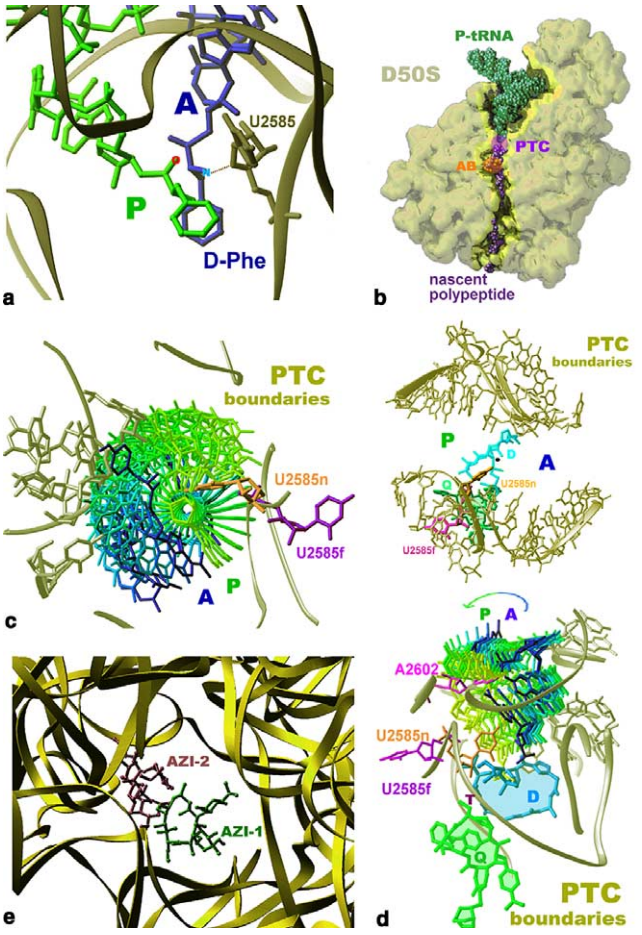

Fig. 3. (a) A presumed D-amino acids position. The figure provides the structural basis for the elimination of D-amino acid incorporation. It shows the results of an attempt to model D-phenylalanine within the PTC, by overlapping a D-isomer on the ASM 3′end, and highlights the possible contacts of the D-aminoacid model with U2585. (b) A section through the large ribosomal subunit (in yellow-gray), at the height of the ribosomal tunnel. P-site tRNA was docked based on its position within the entire ribosome [3] and the nascent chain has been modeled as in [12]. The approximate positions of the PTC and of the site targeted by macrolides antibiotics are highlighted in violet and orange, respectively. (c) The conformational alteration of U2585 induced by binding of dalfopristin, the S_A component of Synercid©, viewed from the tunnel into the PTC (similar to Fig. 2(b)). The positions of U2585 in the native (U2585n) and the complex with the antibiotics dalfopristin (D) flipped (U2585f) orientation are marked. (d) Two orthogonal views of the PTC and the tunnel entrance showing the structural basis for the Synercid© synergetic effect. Dalfopristin (D) and Quinupristin (Q) are colored by cyan and light-green, respectively, and the approximate volume occupied by them is shaded. Note the edge-on view of Dalfopristin in the upper panel. Top: a view similar to that shown in Fig. 2(d), but seen from the opposite side. Bottom: a view approximately parallel to the symmetry axis, showing also a simulation of the rotation (performed as for Fig. 2(b)) of A-site tRNA-3′end aminoacylated by alanine. (e) The positions of the two molecules of azithromycin (called AZI-1 and AZI-2) bound simultaneously to the ribosome tunnel. The backbone of the rRNA is shown as yellow ribbons.

high degree of cooperativity [41,42] and prolonged activity, persisting after drug removal [43,44]. Among them is Synercid®, a recently approved injectable streptogramin with excellent activity against gram-positive bacteria [45], which is composed of 30:70 combination of dalfopristin (S_A) and quinupristin (S_B),

The crystal structure of D50S complex, with clinically relevant concentrations of Synercid®, showed that quinupristin binds to the exit tunnel [15] to the crevice favored by the common macrolides. Its binding mode is, similar, albeit not identical, to those of common macrolides [7]. Nevertheless, despite its slight inclination towards the tunnel wall (Fig. 3(d)), which rationalizes its reduced antibacterial effects in the absence of its S_A mate, it is involved in most of the macrolide-typical interactions of its desosamine sugar with A2058 and its vicinity [15]. This binding mode is in accord with the competition between erythromycin and S_B compounds [46] and with the common resistance mechanisms to both classes of antibiotics, namely methylation or mutation of A2058 (reviewed in [39,47]). The interactions of the S_B component of Synercid® with A2058 shed light on the absence of significant binding of S_B to the large ribosomal subunit from the Archaeon *H. marismortui* [9], as this species possesses the typical eukaryotic G in position 2058, rather than the common eubacterial A.

The second Synercid® component, dalfopristin, binds to the PTC by a network of hydrophobic interactions in a position almost overlapping chloramphenicol binding site [7], consistent with S_A interference with substrate binding, reported two decades ago [48]. However, contrary to chloramphenicol, dalfopristin binding induces remarkable alterations in the PTC [15], consistent with conclusions based on biochemical data [49,50]. The most significant dalfopristin induced conformational change, caused by space exclusion, is a 180° flip of the base of nucleotide U2585 (Figs. 3(b) and (c)), one of the anchors of the rotatory motion. In the native structure, this base points into the PTC, at the exit tunnel entrance. In its flipped orientation U2585 interacts with C2606 and G2588, leading to a fairly stable alteration of the P-region of the PTC, reasoning its severe effect on P-site tRNA proper positioning [40]. Interestingly, though the inversion of U2585 orientation appears to be crucial for S_A binding, U2585 conformation is hardly changed in H50S-streptogramin complex [51]. This finding correlates well with the inherent differences in PTC conformations in H50S [5] and in eubacterial ribosomes [3,4], and accords with the suggestion that chloramphenicol and streptogramins exploit different inhibitory mechanisms on archea compared to eubacteria [49].

Despite the relative stability of U2585 flipped orientation in the presence of dalfopristin, it is conceivable that its natural interactions with the PTC and the tRNA-3′ends could compete with those provided in the flipped orientation. This competition should cause ejection or re-localization of the drug, justifying the reduced antibacterial activity observed for binding dalfopristin by itself, as well as the need for additional contributions in order to achieve significant antibacterial activity (Fig. 3(c)). Quinupristin binding could supply this need, since it should block the relocation or the ejection of dalfopristin, thus fixing U2585 in its flipped orientation while eliminating nascent peptides progression. Importantly, in the structure of its complex with D50S both Synercid® components interact with each other and share contacts with nucleotide A2062 [15], consistent with observations made in solution [50,52]. It appears, therefore, that confining U2585 to its flipped conformation, by itself or as a consequence of the interactions between the two Synercid® components via the shared contacts with A2062, is the main contributor to Synercid® synergetic effect in bactericidal activity as well as for its prolonged activity.

Dual drug binding leading to enhanced activity was observed also in D50S complex with azithromycin [14], a 15-members macrolides developed to combat resistance [53]. Similar to all macrolides studied so far, azithromycin exerts its antimicrobial activity by blocking the exit tunnel. Contrary to the others, two azithromycin molecules, interacting with each other, bind simultaneously to the ribosome (Fig. 3(e)). Between the two bound molecules, one is located in a position and orientation similar to that observed for erythromycin [7], and the second reaches the other side of the tunnel, where it interacts with ribosomal proteins L4 and L22, both implied in macrolide resistance [54]. The two azithromycin molecules are in direct contact, and crystallographic criteria indicate a stronger binding of the second [14]. This mode of binding was originally thought to be specific for *D. radiodurans*, since one of the contacts of the second azithromycin involves a non-conserved glycine (gly60) of protein L4 [7]. However, since azithromycin interacts with the backbone of gly60, and since computer simulations showed that various side-chains could be accommodated in a way that would not perturb these interactions, it is likely that two azithromycin molecules can bind simultaneously only to *D. radiodurans*. Likewise, the second azithromycin, which is located in proximity to protein L22 β-hairpin tip, could induce a swing of the β-hairpin across the tunnel, similar to the action of troleandomycin [12].

Further analysis of azithromycin binding mode, including modeling and energetic considerations accompanied with new findings showing dual and triple binding for several members of the macrolide–ketolide family (data not shown), indicated rather high probability for similar binding modes in various ribosomes, including those of pathogenic bacteria. Our studies show that species likely to bind simultaneously two azithromycin molecules include *Haemophilus influenzae*, *E. coli*, *Mycobacterium tuberculosis*, *Helicobacter pylori*, *Mycoplasma pneumoniae* and *Mycobacterium leprae* (A. Sittner and A. Bashan, to be published).

5. Conclusions

We have shown that the ribosomal elaborate architecture is designed for navigating and controlling peptide-bond formation and continuous amino-acid polymerization, thus confirming that the ribosome contributes positional, rather than chemical catalysis. Our conclusions are based on the linkage between internal ribosomal symmetrical framework and the orientation of the tRNA substrates, as well as on the revelation of a ribosomal pattern outlining the exact path taken by tRNA-3′end during A- to P-site passage.

Our analysis of the spectacular ribosomal architecture rationalizes several seemingly contradictory findings: (a) a sizable symmetry related region within the giant asymmetrical ribosome, which could be rationalized by the requirement for mutual substrate stereochemistry suitable for the formation of the peptide bond; (b) PTC mobility and tolerance vs. the exact localization of the ribosomal substrates, found to be manda-

tory for smooth peptide bond formation. The requirement for substrate precise orientation explains the location of the PTC at the bottom of a deep cavity, as the upper rim of this cavity provides the remote interactions that govern substrate's placement; (c) single peptide bond formation by protein-free 23S RNA vs. the significant contribution of protein L2 to efficient amino acid polymerization. Thus, apart from providing the structural basis for L2 evolutionary conservation, these findings emphasize the dual missions of ribosomal catalysis: peptide bond formation and amino acid polymerization.

Finally, we identified two universally conserved multi-functional PTC nucleotides that do not obey the ribosomal twofold symmetry and possess incredible dynamics, enabling their participation in peptide bond formation. One of them, A2602, is suggested to facilitate PTC-substrate conformational rearrangements, and propel the A-site tRNA-3′end rotatory motion. The second, U2585, is anchoring this motion, and seems to be involved in tunneling nascent proteins into their exit tunnel as well as in D-amino acids discrimination. U2585 plays also a key role in acquiring the synergetic enhancement of the two Synercid® components. Thus, upon the binding of Synercid® streptogramin$_A$ component, U2585 flips out of the PTC into a non-productive orientation, which becomes almost completely irreversible upon the binding of the streptogramin$_B$ component of Synercid®. Extending our studies on synergistic effects originating from interactions between two antibiotic compounds, we propose that enhanced antibiotic effect could be correlated with the dual binding of the same antibiotic compound. Thus, the improved antimicrobial properties of azithromycin, which were originally attributed to the specific properties of *D. radiodurans*, could be extended, by careful simulation, to many other species, including pathogenic bacteria.

Acknowledgements: Thanks are due to J.M. Lehn, P. Ahlberg, M. Lahav, H. Gilon, H. Rosenberg and W. Bennett for critical discussions, to F. Franceschi and P. Fucini for supplying crystals and to M. Peretz, C. Liebe, A. Wolff, R. Albrecht and M. Laschever, for contributing to different stages of this work. X-ray diffraction data were collected at ID19/SBC/APS/ANL and ID14/ESRF-EMBL. Support was provided by US National Inst. of Health (GM34360), the German Ministry for Science & Technology (BMBF05-641EA), Kimmelman Center for Macromolecular Assemblies, and LR5-02 (to R.B.). A.Y. holds the Helen and Martin Kimmel Professorial Chair.

References

[1] Schluenzen, F., Tocilj, A., Zarivach, R., Harms, J., Gluehmann, M., Janell, D., Bashan, A., Bartels, H., Agmon, I., Franceschi, F. and Yonath, A. (2000) Cell 102, 615–623.
[2] Wimberly, B.T., Brodersen, D.E., Clemons Jr., W.M., Morgan-Warren, R.J., Carter, A.P., Vonrhein, C., Hartsch, T. and Ramakrishnan, V. (2000) Nature 407, 327–339.
[3] Yusupov, M.M., Yusupova, G.Z., Baucom, A., Lieberman, K., Earnest, T.N., Cate, J.H. and Noller, H.F. (2001) Science 292, 883–896.
[4] Harms, J., Schluenzen, F., Zarivach, R., Bashan, A., Gat, S., Agmon, I., Bartels, H., Franceschi, F. and Yonath, A. (2001) Cell 107, 679–688.
[5] Ban, N., Nissen, P., Hansen, J., Moore, P.B. and Steitz, T.A. (2000) Science 289, 905–920.
[6] Nissen, P., Hansen, J., Ban, N., Moore, P.B. and Steitz, T.A. (2000) Science 289, 920–930.
[7] Schluenzen, F., Zarivach, R., Harms, J., Bashan, A., Tocilj, A., Albrecht, R., Yonath, A. and Franceschi, F. (2001) Nature 413, 814–821.
[8] Schmeing, T.M., Seila, A.C., Hansen, J.L., Freeborn, B., Soukup, J.K., Scaringe, S.A., Strobel, S.A., Moore, P.B. and Steitz, T.A. (2002) Nat. Struct. Biol. 9, 225–230.
[9] Hansen, J.L., Ippolito, J.A., Ban, N., Nissen, P., Moore, P.B. and Steitz, T.A. (2002) Mol. Cell 10, 117–128.
[10] Hansen, J.L., Schmeing, T.M., Moore, P.B. and Steitz, T.A. (2002) Proc. Natl. Acad. Sci. USA 99, 11670–11675.
[11] Bashan, A., Agmon, I., Zarivach, R., Schluenzen, F., Harms, J., Berisio, R., Bartels, H., Franceschi, F., Auerbach, T., Hansen, H.A.S., Kossoy, E. Kessler, M. and Yonath, A. (2003) Mol. Cell. 11, 91–102.
[12] Berisio, R., Schluenzen, F., Harms, J., Bashan, A., Auerbach, T., Baram, D. and Yonath, A. (2003) Nat. Struct. Biol. 10, 366–370.
[13] Berisio, R., Harms, J., Schluenzen, F., Zarivach, R., Hansen, H.A.S., Fucini, P. and Yonath, A. (2003) J. Bacteriol. 185, 4276–4279.
[14] Schluenzen, F., Harms, J.M., Franceschi, F., Hansen, H.A., Bartels, H., Zarivach, R. and Yonath, A. (2003) Structure 11, 329–338.
[15] Harms, J.M, Schluenzen, F., Fucini, Bartels, H. and Yonath, A. (2004) BMC Biol. (in press).
[16] Bashan, A., Zarivach, R., Schluenzen, F., Agmon, I., Harms, J., Auerbach, T., Baram, D., Berisio, R., Bartels, H., Hansen, H.A., Fucini, P., Wilson, D., Peretz, M., Kessler, M. and Yonath, A. (2003) Biopolymers 70, 19–41.
[17] Agmon, I., Auerbach, T., Baram, D., Bartels, H., Bashan, A., Berisio, R., Fucini, P., Hansen, H.A., Harms, J., Kessler, M., Peretz, M., Schluenzen, F., Yonath, A. and Zarivach, R. (2003) Eur. J. Biochem. 270, 2543–2556.
[18] Agmon, I., Bashan, A., Zarivach, R., Yonath, A. (2004) submitted.
[19] Moore, P.B. and Steitz, T.A. (2003) RNA 9, 155–159.
[20] Yonath, A. (2003) Biol. Chem. 384, 1411–1419.
[21] Yonath, A. (2003) Chem. Biol. Chem. 4, 1008–1017.
[22] Samaha, R.R., Green, R. and Noller, H.F. (1995) Nature 377, 309–314.
[23] Fujiwara, S., Lee, S.G., Haruki, M., Kanaya, S., Takagi, M. and Imanaka, T. (1996) FEBS Lett. 394, 66–70.
[24] Uhlein, M., Weglohner, W., Urlaub, H. and Wittmann-Liebold, B. (1998) Biochem. J. 331, 423–430.
[25] Nitta, I., Kamada, Y., Noda, H., Ueda, T. and Watanabe, K. (1998) Science 281, 666–669.
[26] Kim, D.F. and Green, R. (1999) Mol. Cell. 4, 859–864.
[27] Miskin, R., Zamir, A. and Elson, D. (1968) Biochem. Biophys. Res. Commun. 33, 551–557.
[28] Vogel, Z., Vogel, T., Zamir, A. and Elson, D. (1971) J. Mol. Biol. 60, 339–346.
[29] Zamir, A., Miskin, R., Vogel, Z. and Elson, D. (1974) Methods Enzymol. 30, 406–426.
[30] Bayfield, M.A., Dahlberg, A.E., Schulmeister, U., Dorner, S. and Barta, A. (2001) Proc. Natl. Acad. Sci. USA 98, 10096–10101.
[31] Yonath, A. (2002) Annu. Rev. Biophys. Biomol. Struct. 31, 257–273.
[32] Zarivach, R., Bashan, A., Berisio, R., Harms, J., Auerbach, T., Schluenzen, F., Bartels, H., Baram, D., Pyetan, E., Sittner, A. Amit, M., Hansen, H.A.S., Kessler, M., Liebe, C., Wolff, A., Agmon, I. and Yonath, A. (2004) J. Phys. Org. Chem. (in press).
[33] Dedkova, L.M., Fahmi, N.E., Golovine, S.Y. and Hecht, S.M. (2003) J. Am. Chem. Soc. 125, 6616–6617.
[34] Green, R., Samaha, R.R. and Noller, H.F. (1997) J. Mol. Biol. 266, 40–50.
[35] Wower, J., Kirillov, S.V., Wower, I.K., Guven, S., Hixson, S.S. and Zimmermann, R.A. (2000) J. Biol. Chem. 275, 37887–37894.
[36] Bocchetta, M., Xiong, L. and Mankin, A.S. (1998) Proc. Natl. Acad. Sci. USA 95, 3525–3530.
[37] Porse, B.T., Thi-Ngoc, H.P. and Garrett, R.A. (1996) J. Mol. Biol. 264, 472–483.
[38] Moazed, D. and Noller, H.F. (1991) Proc. Natl. Acad. Sci. USA 88, 3725–3728.
[39] Auerbach, T., Bashan, A., Harms, J., Schluenzen, F., Zarivach, R., Bartels, H., Agmon, I., Kessler, M., Pioletti, M., Franceschi, F. and Yonath, A. (2002) Curr. Drug Targets – Infect. Disord. 2, 169–186.
[40] Cocito, C., Di Giambattista, M., Nyssen, E. and Vannuffel, P. (1997) J. Antimicrob. Chemother. 39, 7–13.

[41] Allignet, J., Aubert, S., Morvan, A. and el Solh, N. (1996) Antimicrob. Agents Chemother. 40, 2523–2528.
[42] Malbruny, B., Canu, A., Bozdogan, B., Fantin, B., Zarrouk, V., Dutka-Malen, S., Feger, C. and Leclercq, R. (2002) Antimicrob. Agents Chemother. 46, 2200–2207.
[43] Nyssen, E., Di Giambattista, M. and Cocito, C. (1989) Biochim. Biophys. Acta 1009, 39–46.
[44] Parfait, R. and Cocito, C. (1980) Proc. Natl. Acad. Sci. USA 77, 5492–5496.
[45] Nakashio, S., Iwasawa, H., Iino, S. and Shimada, J. (1997) Jpn. J. Antibiot. 50, 844–853.
[46] Parfait, R., Di Giambattista, M. and Cocito, C. (1981) Biochim. Biophys. Acta 654, 236–241.
[47] Pereyre, S., Gonzalez, P., De Barbeyrac, B., Darnige, A., Renaudin, H., Charron, A., Raherison, S., Bebear, C. and Bebear, C.M. (2002) Antimicrob. Agents Chemother. 46, 3142–3150.
[48] Chinali, G., Moureau, P. and Cocito, C.G. (1984) J. Biol. Chem. 259, 9563–9568.
[49] Porse, B.T. and Garrett, R.A. (1999) J. Mol. Biol. 286, 375–387.
[50] Rodriguez-Fonseca, C., Amils, R. and Garrett, R.A. (1995) J. Mol. Biol. 247, 224–235.
[51] Hansen, J.L., Moore, P.B. and Steitz, T.A. (2003) J. Mol. Biol. 330, 1061–1075.
[52] Porse, B.T., Kirillov, S.V., Awayez, M.J. and Garrett, R.A. (1999) RNA 5, 585–595.
[53] Bright, G.M., Nagel, A.A., Bordner, J., Desai, K.A., Dibrino, J.N., Nowakowska, J., Vincent, L., Watrous, R.M., Sciavolino, F.C. and English, A.R., et al. (1988) J. Antibiot. 41, 1029–1047.
[54] Wittmann, H.G., Stoffler, G., Apirion, D., Rosen, L., Tanaka, K., Tamaki, M., Takata, R., Dekio, S. and Otaka, E.. (1973) Mol. Gen. Genet. 127, 175–189.